

# Switchable Dual-Band 170/420 MHz VCO for Handset Cellular Applications



APN1007

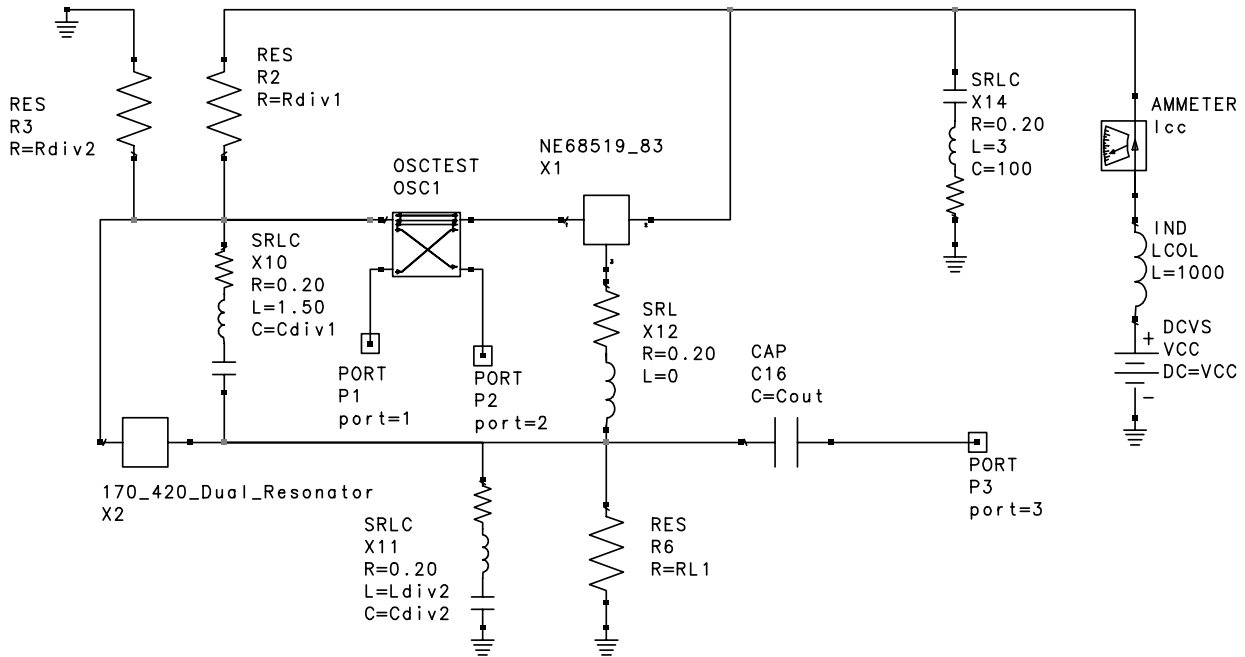
## Introduction

Modern multiband cellular handsets use multiple voltage control oscillator (VCO) functions to accommodate the many down/up conversions in the intermediate frequency (IF) portion. Using separate VCOs would cause a substantial increase in cost and size of the radio frequency (RF) section. This component overload can be resolved by implementing band switchable VCOs.

In many commercial switchable VCOs the reactive elements in the tank circuit are switched. This function is usually performed with PIN diodes. The disadvantage of this solution is that in the closed circuit state ("diode on" state) there is  $V_{CC}$  current flowing through the diode. This  $V_{CC}$  current carries electrical noise which directly

modulates the VCO frequency. Therefore, the noise spectrum may grow significantly beyond the PLL filter range. This type of switching also limits the switching to within 10–15 percent of the center frequency, due to the strong effect of PIN diode series resistance on the tank circuit losses, increasing phase noise.

In this paper, we describe a new switchable VCO solution which employs switching between separate tank circuits. This reduces the effect of PIN diode series resistance on VCO noise performance and results in virtually unlimited switching range and individual optimization of each tank circuit.



**170\_420\_Dual\_Resonator**

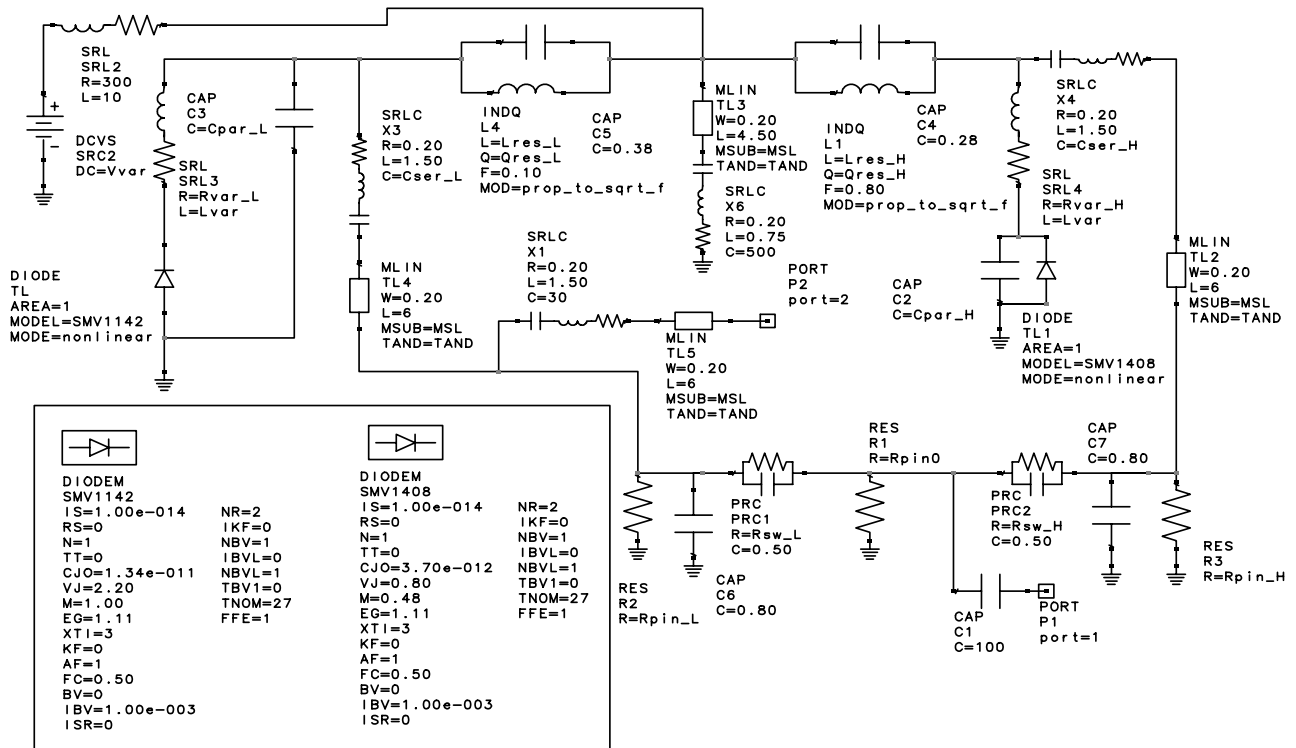


Figure 1. VCO Model

## The VCO Model

In the circuit schematic in Figure 1, a traditional Colpitts structure, the varactors are connected as shunt capacitors. Tank inductors,  $L_4$  and  $L_1$ , providing DC bias to the varactors, are shunted to ground at the common point with capacitor  $X_6$ . Inductors  $L_4$  and  $L_1$  are modeled as lossy elements (with  $Q = 25$  at 100 MHz) in parallel with capacitors  $C_5$  and  $C_4$  of 0.38 and 0.28 pF respectively. This is typical for multilayer inductors of style 0603 (60 x 30 mil footprint), (TOKO Coils and Filters catalogue). The tank inductor values of 12 and 56 nH were optimized to fit the desired 170 MHz and 420 MHz frequency bands. Capacitor  $X_6$  is modeled as a series RLC network with the length of transmission line  $TL_3$ , appropriated to its position on the layout (see later). Series capacitive reactances,  $X_3$  and  $X_4$  are also modeled as lossy series RLC networks, with their appropriate layout-specific transmission lines,  $TL_4$  and  $TL_2$ . Shunt capacitors,  $C_7$  and  $C_6$ , are due to the effects of multiple components pads. The DC bias resistance,  $SRL_2$ , was chosen relatively small, 300  $\Omega$ , to avoid significant thermal noise generation.

The PIN diodes were modeled as parallel RC networks,  $PRC_1$  and  $PRC_2$ , with switching resistances  $R_{SW\_L}$  and  $R_{SW\_H}$ , in the low band and high band branches respectively. The appropriate biasing resistors are shown as shunt elements to ground,  $R_2$ ,  $R_1$  and  $R_3$ , respectively. The truth table showing the values of  $R_{SW\_L}$  and  $R_{SW\_H}$  for the appropriate low/high switching is shown in Table 1.

$R_{SW\_L}$	$R_{SW\_H}$	State
3 $\Omega$	3000 $\Omega$	Low Band
3000 $\Omega$	3 $\Omega$	High Band

**Table 1. Truth Table**

Capacitor  $X_1$  improves the low band matching of the tank circuit, insignificantly affecting high band performances of the tank, because of the high resistance of  $PRC_1$  in the “low band” state. This component may be removed for narrower frequency switching.

The Colpitts feedback capacitances,  $C_{DIV1} = 20$  pF and  $C_{DIV2} = 15$  pF, were optimized to provide a reasonable power response over the switching range.

The NEC NE68519 transistor was selected for its high gain and low noise performance. The output is supplied from the emitter load resistance,  $RL_1$  through the 20 pF coupling capacitor, modeled as a series  $SLC_1$  component.

Figure 2 shows the Libra Test Bench. In the test bench we define an open loop gain,  $K_u = V_{Out}/V_{In}$ , as a ratio of voltage phasors at input and output ports of an OSCTEST component. Defining the oscillation point balances the input (loop) power to provide zero gain for a zero loop phase shift. Once the oscillation point is defined, the frequency and output power may be measured. We don't recommend using the OSCTEST2 component for the closed loop analysis, since it may not always converge and does not allow clear insight into the understanding of VCO behavior. This is considered an advantage of modeling over a purely experimental study.

Figure 3 shows the Default Bench. The variables used for more convenient tuning during performance analysis and optimization are listed in a “variables and equations” component.

## SMV1142-011 and SMV1408-011 SPICE Models

SPICE models for the SMV1142-011 and SMV1408-011 varactor diodes defined for the Libra IV environment, are shown in Figure 4 and Figure 5 with a description of the parameters employed.

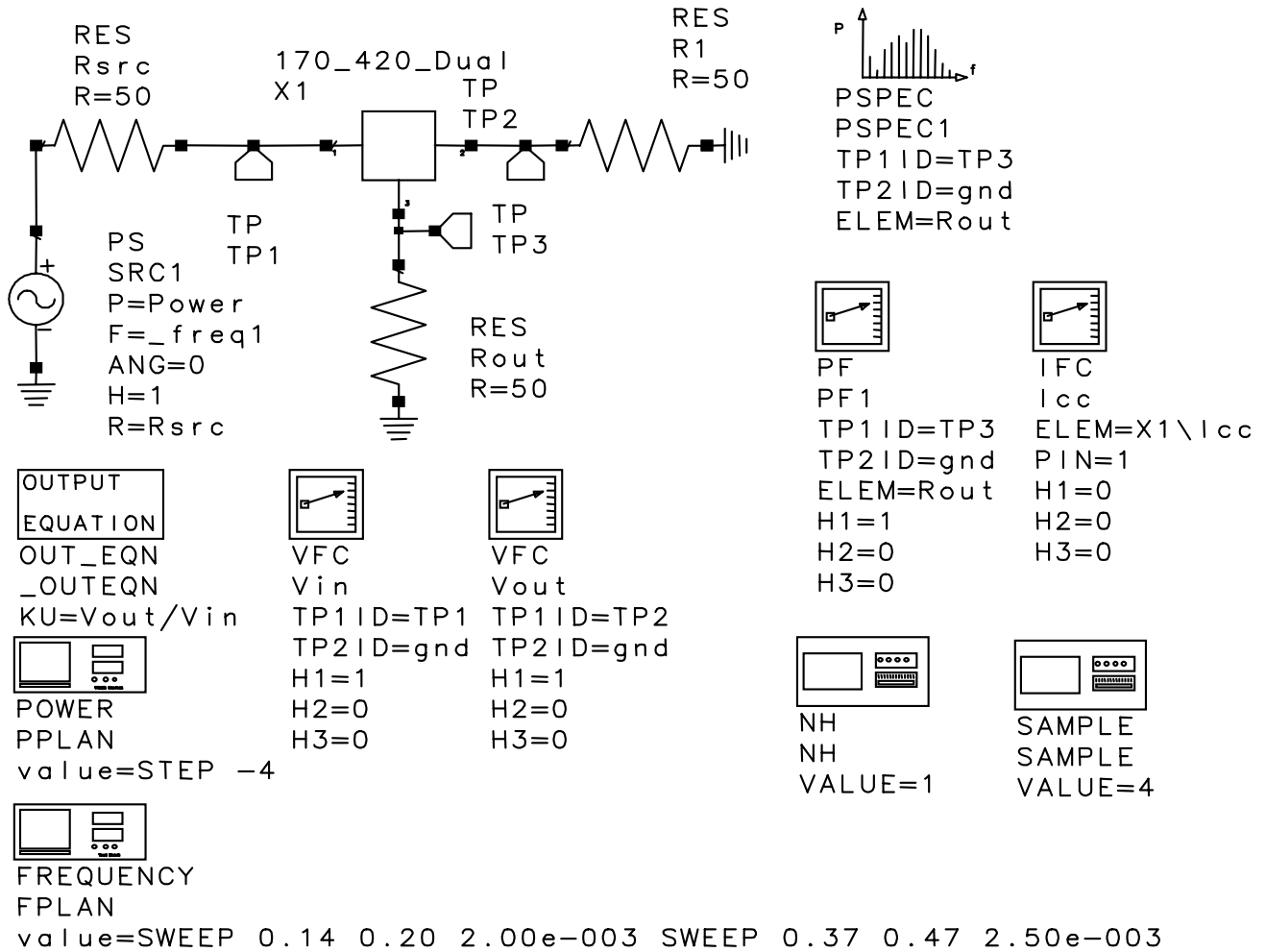


Figure 2. Libra Test Bench

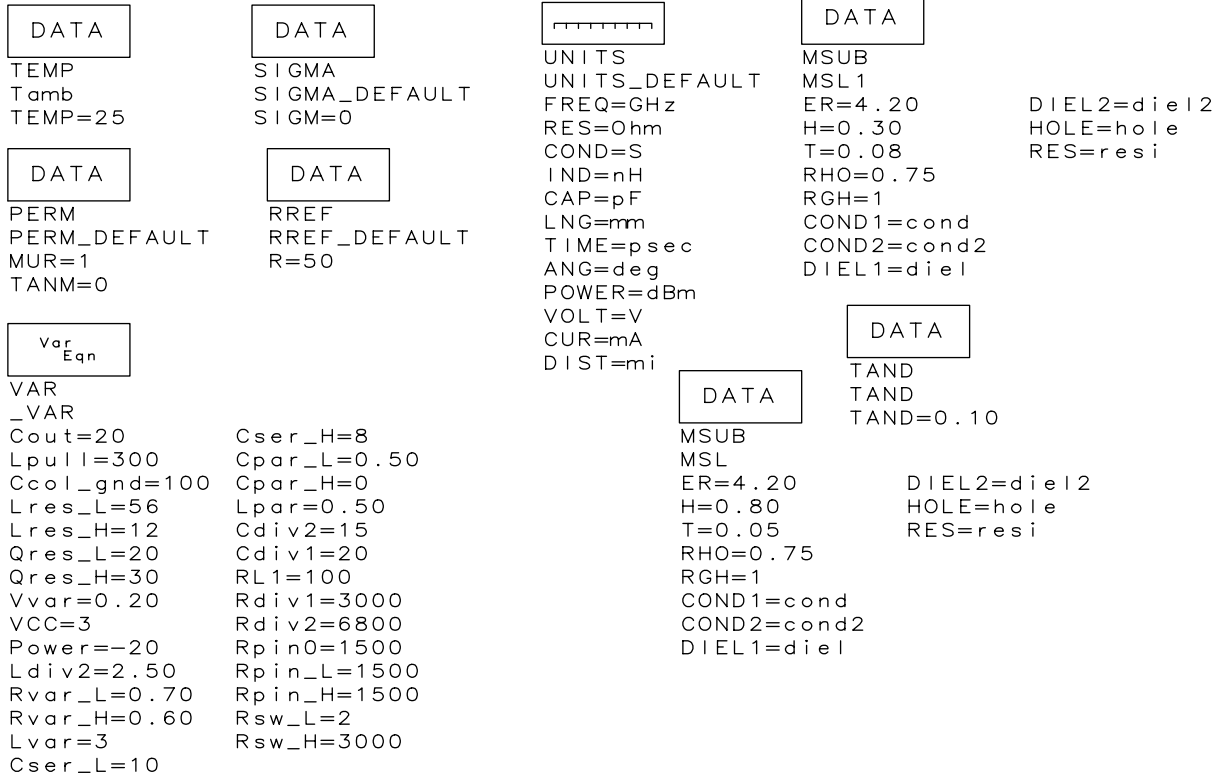


Figure 3. Default Bench

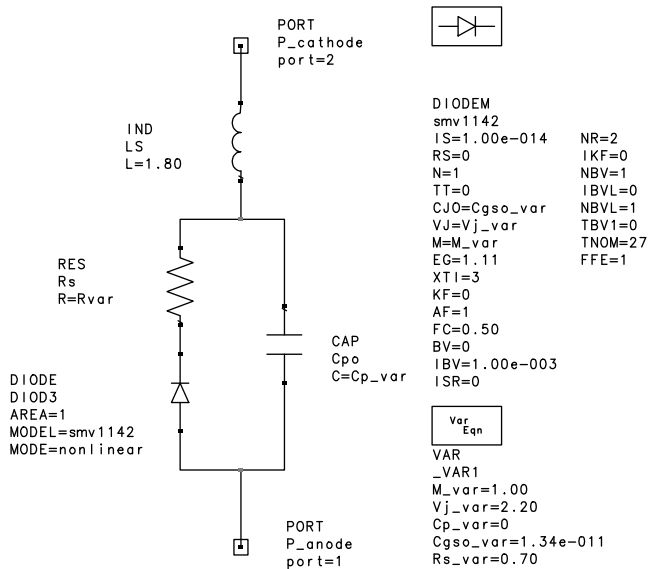


Figure 4. SPICE Model for SMV1142-011

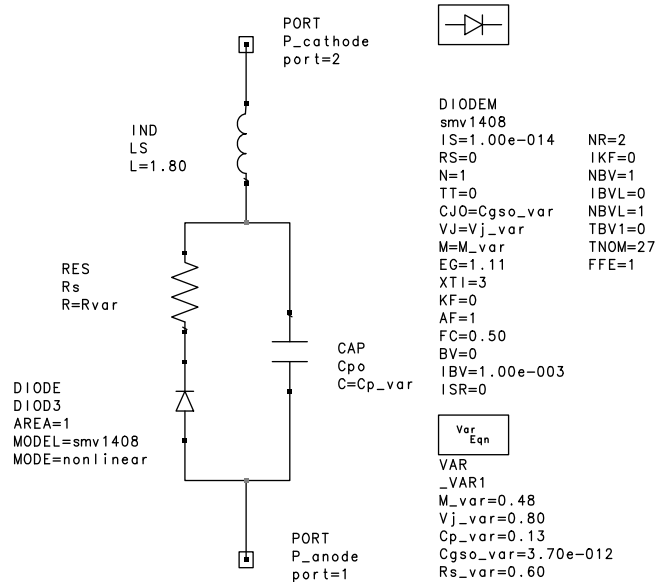


Figure 5. SPICE Model for SMV1408-011

Parameter	Description	Unit	Default
I <sub>S</sub>	Saturation current (with N, determine the DC characteristics of the diode)	A	1e-14
R <sub>S</sub>	Series resistance	Ω	0
N	Emission coefficient (with I <sub>S</sub> , determines the DC characteristics of the diode)	-	1
TT	Transit time	S	0
C <sub>JO</sub>	Zero-bias junction capacitance (with V <sub>J</sub> and M, defines nonlinear junction capacitance of the diode)	F	0
V <sub>J</sub>	Junction potential (with V <sub>J</sub> and M, (C <sub>JO</sub> and M) defines nonlinear junction capacitance of the diode)	V	1
M	Grading coefficient (with V <sub>J</sub> and M, (C <sub>JO</sub> and V <sub>J</sub> ) defines nonlinear junction capacitance of the diode)	-	0.5
E <sub>G</sub>	Energy gap (with XTI, helps define the dependence of I <sub>S</sub> on temperature)	EV	1.11
XTI	Saturation current temperature exponent (with E <sub>G</sub> , helps define the dependence of I <sub>S</sub> on temperature)	-	3
KF	Flicker noise coefficient	-	0
AF	Flicker noise exponent	-	1
FC	Forward-bias depletion capacitance coefficient	-	0.5
B <sub>V</sub>	Reverse breakdown voltage	V	Infinity
I <sub>BV</sub>	Current at reverse breakdown voltage	A	1e-3
ISR	Recombination current parameter	A	0
NR	Emission coefficient for ISR	-	2
IKF	High-injection knee current	A	Infinity
NBV	Reverse breakdown ideality factor	-	1
IBVL	Low-level reverse breakdown knee current	A	0
NBVL	Low-level reverse breakdown ideality factor	-	1
T <sub>NOM</sub>	Nominal ambient temperature at which these model parameters were derived	°C	27
FFE	Flicker noise frequency exponent		1

Table 2. Model Parameters

Table 2 describes the model parameters. It shows default values appropriate for silicon varactor diodes that may be used by the Libra IV simulator.

According to the SPICE model in Figures 4 and 5, the varactor capacitance, C<sub>V</sub>, is a function of the applied reverse DC voltage, V<sub>R</sub>, and may be expressed as follows:

$$C_V = \frac{C_{JO}}{\left(1 + \frac{V_{VAR}}{V_J}\right)^M} + C_P$$

This equation is a mathematical expression of the capacitance characteristic. The model is accurate for abrupt junction varactors (like Alpha’s SMV1408). The model is less accurate for hyperabrupt junction varactors because the coefficients are dependent on applied voltage. To make the above equation work better for the hyperabrupt varactors, the coefficients were optimized for the best capacitance vs. voltage fit as shown in Table 3 and Figure 6.

Note: In the Libra model shown in Figure 6, C<sub>P</sub> is given in picofarads, while C<sub>GO</sub> is given in farads to comply with the default unit system used in Libra.

Part Number	C <sub>JO</sub> (pF)	M	V <sub>J</sub> (V)	C <sub>P</sub> (pF)	R <sub>S</sub> (Ω)	L <sub>S</sub> (nH)
SMV1142-011	13.4	1	2.2	0	0.7	1.8
SMV1408-011	21	25	68	0.13	0.6	1.8

Table 3. Optimized Coefficients for Capacitance vs. Voltage

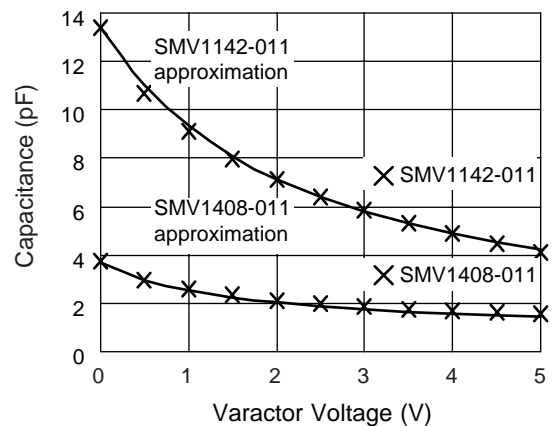


Figure 6. Capacitance vs. Voltage

## VCO Design, Materials, Layout and Performance

Figure 7 shows the VCO circuit diagram.

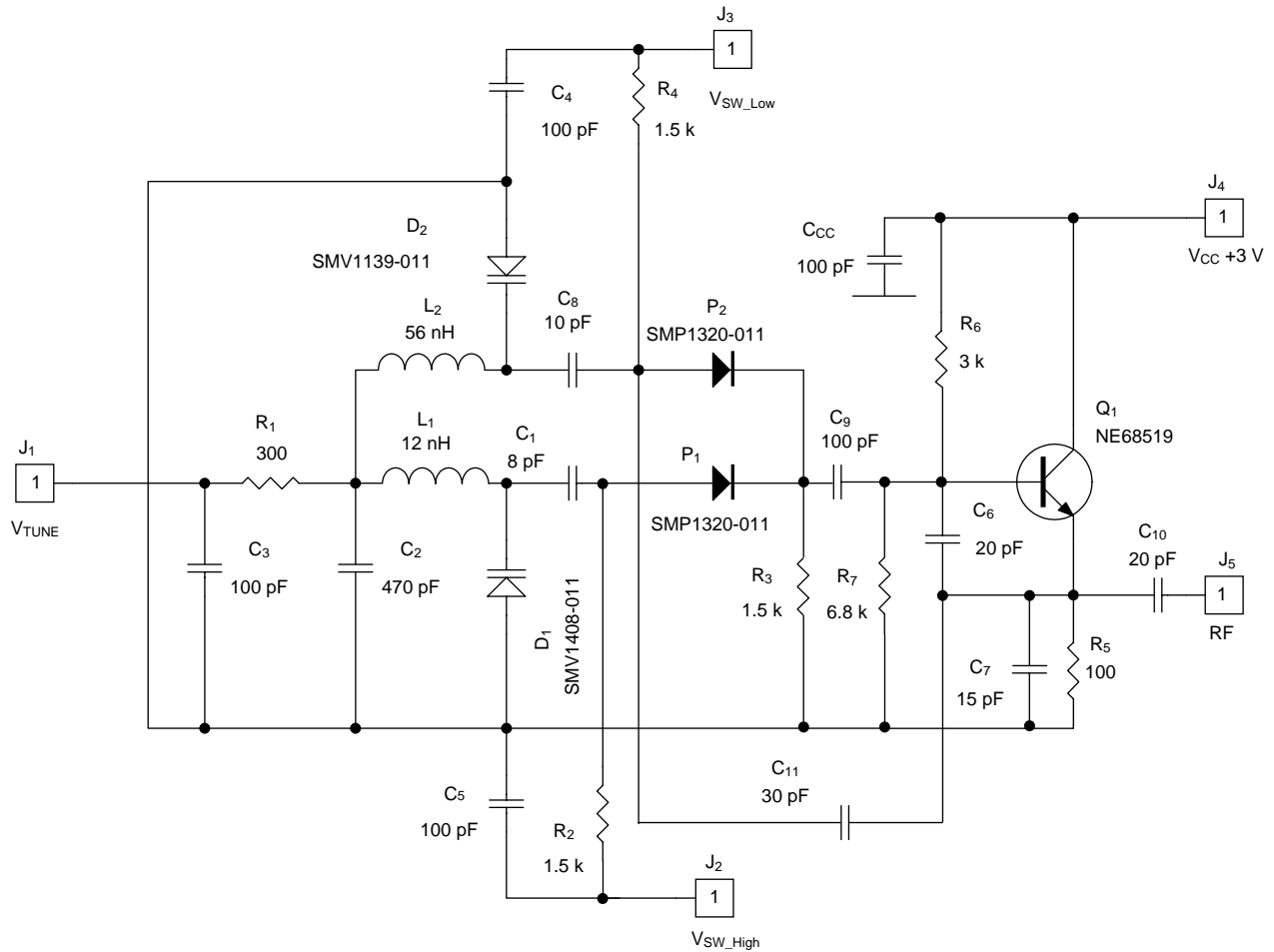


Figure 7. VCO Circuit Diagram

Table 4 shows the bill of materials used.

Designator	Value	Part Number	Footprint	Manufacturer
C <sub>1</sub>	8 pF	0603AU8R0JAT9	0603	AVX
C <sub>2</sub>	470 pF	0603AU471JAT9	0603	AVX
C <sub>3</sub>	100 pF	0603AU101JAT9	0603	AVX
C <sub>4</sub>	100 pF	0603AU101JAT9	0603	AVX
C <sub>5</sub>	100 pF	0603AU101JAT9	0603	AVX
C <sub>6</sub>	20 pF	0603AU200JAT9	0603	AVX
C <sub>7</sub>	15 pF	0603AU150JAT9	0603	AVX
C <sub>8</sub>	10 pF	0603AU100JAT9	0603	AVX
C <sub>9</sub>	100 pF	0603AU101JAT9	0603	AVX
C <sub>10</sub>	20 pF	0603AU200JAT9	0603	AVX
C <sub>11</sub>	30 pF	0603AU300JAT9	0603	AVX
C <sub>CC</sub>	100 pF	0603AU101JAT9	0603	AVX
L <sub>1</sub>	12 nH	LL1608-F12NS	0603	TOKO
L <sub>2</sub>	56 nH	LL1608-F56NS	0603	TOKO
R <sub>1</sub>	300	CR10-301J-T	0603	AVX
R <sub>2</sub>	1.5 k	CR10-152J-T	0603	AVX
R <sub>3</sub>	1.5 k	CR10-152J-T	0603	AVX
R <sub>4</sub>	1.5 k	CR10-152J-T	0603	AVX
R <sub>5</sub>	100	CR10-101J-T	0603	AVX
R <sub>6</sub>	3 k	CR10-302J-T	0603	AVX
R <sub>7</sub>	6.8 k	CR10-682J-T	0603	AVX
D <sub>1</sub>	SMV1408-011	SMV1408-011	SOD-323	ALPHA IND.
D <sub>2</sub>	SMV1142-011	SMV1142-011	SOD-323	ALPHA IND.
P <sub>1</sub>	SMP1320-011	SMP1320-011	SOD-323	ALPHA IND.
P <sub>2</sub>	SMP1320-011	SMP1320-011	SOD-323	ALPHA IND.
Q <sub>1</sub>	NE68519	NE68519	SOT-419	NEC

**Table 4. Bill of Materials**

The PCB layout is shown in Figure 8. The board was made of standard, 30 mil thick, FR4 material.

Figures 9 and 10 show the measured performance of this circuit and the simulated results obtained with the model in Figure 8.

In both low and high band states there is good compliance for frequency response. Some of the difference of the measured data and the simulation is probably due to the 5–10 percent variation of circuit capacitances and inductances from their nominal values.

The low band simulated power response was in fair agreement with measured performance, assuming measurement uncertainty of  $\pm 1$  dB. The power response difference of up to 4 dB for the high band may be due to underestimated circuit component losses. For example, a decrease of inductor Q-quality from 30 to 20 decreases output power about 1 dB; an increase in resistance of switching diode from 3 to 6  $\Omega$  will decrease power to about 2 dB.

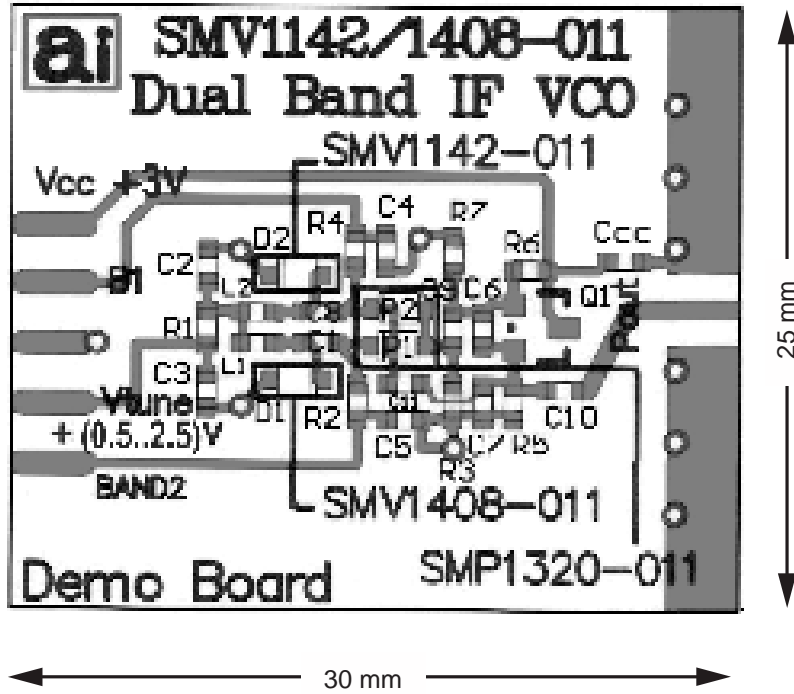


Figure 8. PCB Layout

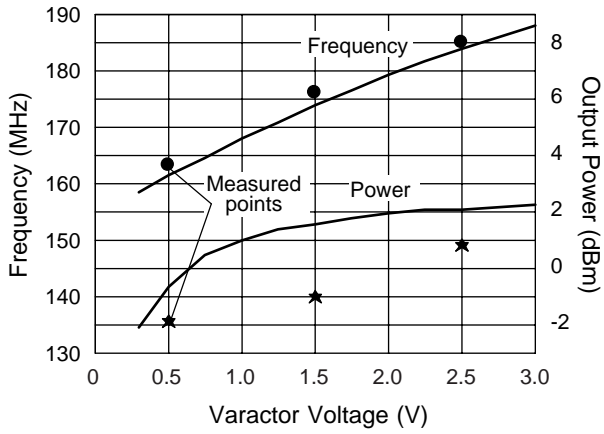


Figure 9. Low Band Measured and Simulated Results

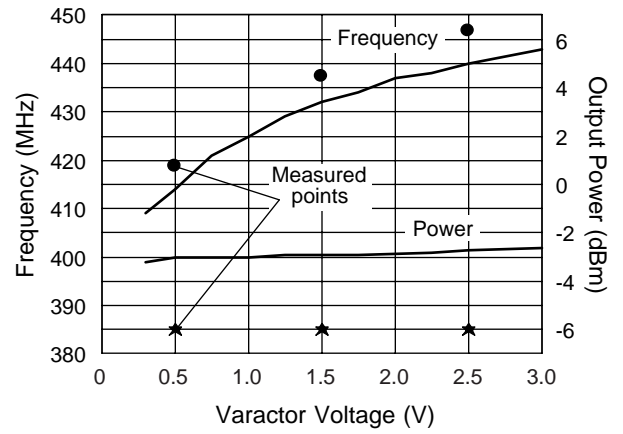


Figure 10. High Band Measured and Simulated Results

Figure 11 shows the phase noise in the high band state vs. frequency offset. It shows better than -95 dBc/Hz at 10 kHz offset. This measurement was made using the PN9000 Phase Noise Test Set, courtesy of Aeroflex Comstron, Plainview, NY ([www.aeroflex.com](http://www.aeroflex.com)).

Phase noise for both bands was measured with the HP8564E spectrum analyzer. At 10 kHz offset the noise was -95 dBc/Hz for both bands. It was expected that phase noise would be better at the low band. The poorer

measured phase noise at the low band may be attributed to the spectrum analyzer method where the internal noise may be too close to the measurement level. It may also be related to the wide-bandwidth matching requirement of the VCO feedback circuit, which makes it difficult to satisfy noise optimums in both bands simultaneously. Our design compromise was to balance noise performance between both bands. In any event, -95 dBc/Hz is considered acceptable for digital cellular applications.

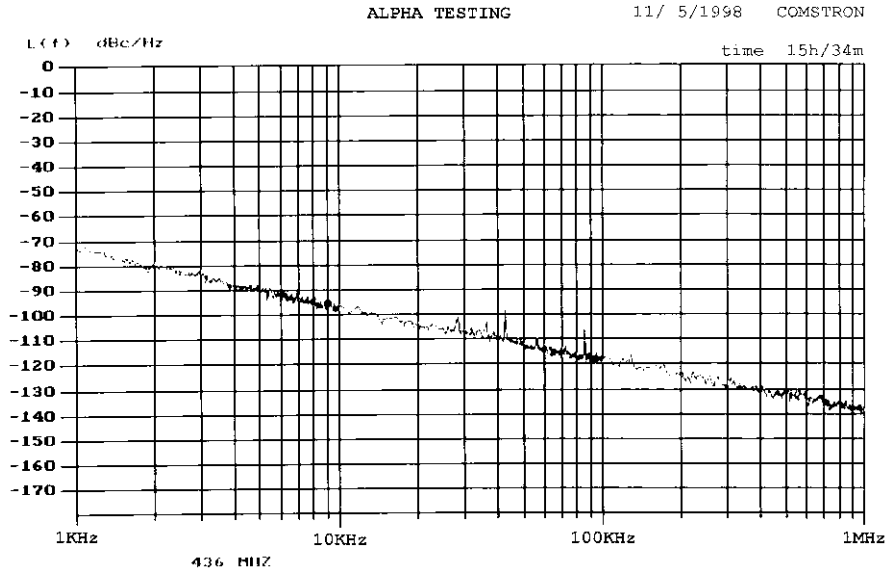


Figure 11. High Band Phase Noise vs. Frequency

## List of Available Documents

1. HF Switchable VCO Simulation Project Files for Libra IV
2. HF Switchable VCO Circuit Schematic and PCB Layout for Protel EDA Client, 1998 Version
3. HF Switchable VCO PCB Gerber Photo-plot Files

(For the availability of the listed materials, please call our applications engineering staff.)

## VCO Related Application Notes

1. Varactor SPICE Models for RF VCO Applications
2. A Colpitts VCO for Wideband (0.95–2.15 GHz) Set-Top TV Tuner Applications
3. A Balanced Wideband VCO for Set-top TV Tuner Applications

© Alpha Industries, Inc., 1999. All rights reserved.